

Nanoparticles can cause DNA damage across a cellular barrier

Gevdeep Bhabra^{1†}, Aman Sood^{1†}, Brenton Fisher¹, Laura Cartwright², Margaret Saunders², William Howard Evans³, Annmarie Surprenant⁴, Gloria Lopez-Castejon⁴, Stephen Mann⁵, Sean A. Davis⁵, Lauren A. Hails⁵, Eileen Ingham⁶, Paul Verkade⁷, Jon Lane⁷, Kate Heesom⁸, Roger Newson⁹ and Charles Patrick Case^{1*}

The increasing use of nanoparticles in medicine has raised concerns over their ability to gain access to privileged sites in the body. Here, we show that cobalt-chromium nanoparticles (29.5 ± 6.3 nm in diameter) can damage human fibroblast cells across an intact cellular barrier without having to cross the barrier. The damage is mediated by a novel mechanism involving transmission of purine nucleotides (such as ATP) and intercellular signalling within the barrier through connexin gap junctions or hemichannels and pannexin channels. The outcome, which includes DNA damage without significant cell death, is different from that observed in cells subjected to direct exposure to nanoparticles. Our results suggest the importance of indirect effects when evaluating the safety of nanoparticles. The potential damage to tissues located behind cellular barriers needs to be considered when using nanoparticles for targeting diseased states.

Nanotechnology is a rapidly advancing discipline with a wide range of applications¹, including those in medicine and surgery². Nanoparticles have a specific capacity for drug loading, high superparamagnetism, efficient photoluminescence and distinctive Raman signatures³, and are therefore important materials in the targeted delivery of imaging agents and anticancer drugs^{4,5}. Potential targets include organs such as the brain, which are normally protected by specialized barriers (such as the blood–brain barrier)⁵. Targeting can be made more effective by systemic exposure of these organs to nanoparticles 20–200 nm in diameter, which avoids their renal filtration and leads to prolonged residence times within the bloodstream³. If these trends in nanomedicine continue, humans will be increasingly exposed to a wide range of synthetic nanomaterials with diverse properties.

The ultrasmall size and unique properties of nanomaterials have led to increasing concerns about their potential toxicity. The current lack of knowledge in this regard has led to an urgent call for the establishment of principles and test procedures to ensure the safe manufacture and use of nanomaterials in the marketplace^{6,7}. Little is known about the clinical risks of exposure or whether nanoparticle exposure may pose a risk to a fetus during pregnancy⁸. Inhalation of nanoparticles or nanotubes is thought to be a risk for cardiorespiratory disease^{9,10}. Although the placenta, lung, gastrointestinal tract and skin have been cited as barriers to many nanomaterials^{11,12}, there is some, albeit conflicting, evidence that nanoparticles from external exposures could translocate to other systemic sites^{6,13}.

In response to these concerns, we explore whether a cellular barrier in the form of a confluent layer of BeWo cells grown on a transwell insert can protect human fibroblasts from damage when indirectly exposed to surgical cobalt–chromium (CoCr) alloy

particles. Humans are exposed internally to CoCr nanoparticles by wear mechanisms associated with metal-on-metal (CoCr) orthopaedic joint replacements^{14,15}. CoCr particles are known to have genotoxic and cytotoxic effects in human tissue culture, causing DNA damage, chromosome aberrations and cell death if they are directly applied above a certain concentration threshold¹⁶. However, no studies have been undertaken to assess the cellular toxicity of nanoparticles when located on the other side of a fully confluent cellular barrier. Here, we use BeWo cells, a human trophoblast choriocarcinoma derived cell line, which has been widely used by others to create a well-established *in vitro* model barrier¹⁷. For example, BeWo cells have been grown as a monolayer on a transwell insert to model the placental transport of amino acids, immunoglobulins, hormones, fatty acids, transferrin and viruses^{17–20}. These studies have focused on the rate and polarity of transport across a barrier of well-defined (single cell) thickness. Because we were exposing our barrier to potentially toxic metals we used a multilayered barrier (see also Fig. 1c in ref. 18) to ensure that even tiny gaps in our barrier would be covered by the underlying cells. In this way we hoped to make sure that we were studying the indirect effects of particle exposure rather than the direct effects of particles that had leaked through the barrier.

Effect of exposure to nanoparticles on fibroblasts

Indirect exposure for 24 h of human fibroblasts to CoCr nanoparticles, CoCr micrometre-sized particles, or aqueous solutions of Cr or Co ions placed behind a confluent layer of BeWo cells grown on a transwell insert (Fig. 1a) caused significant DNA damage to the fibroblasts (Fig. 1b,c (indirect)). The level of damage after indirect exposure when measured with the alkaline comet assay, which

¹Bristol Implant Research Centre, Southmead Hospital, Bristol BS10 5NB, UK, ²Biophysics Research Unit, Department of Medical Physics & Bioengineering, Bristol Haematology & Oncology Centre, University Hospitals Bristol NHS Foundation Trust, Horfield Road, Bristol BS2 8ED, UK, ³Department of Medical Biochemistry and Immunology & Wales Heart Research Institute, Cardiff University, Cardiff CF14 4XN, Wales, ⁴Faculty of Life Sciences, University of Manchester, Michael Smith Building, Oxford Road, Manchester M13 9PT, UK, ⁵School of Chemistry, University of Bristol, Bristol BS8 1TS, UK, ⁶Faculty of Biological Sciences, University of Leeds, Leeds LS2 9JT, UK, ⁷Department of Biochemistry, University of Bristol, Bristol BS8 1TD, UK, ⁸School of Medical Sciences, University of Bristol, Bristol BS8 1TD, UK, ⁹Medical Statistics, National Heart and Lung Institute, Imperial College London SW7 2AZ, UK; [†]These authors contributed equally to this work. *e-mail: c.p.case@bristol.ac.uk

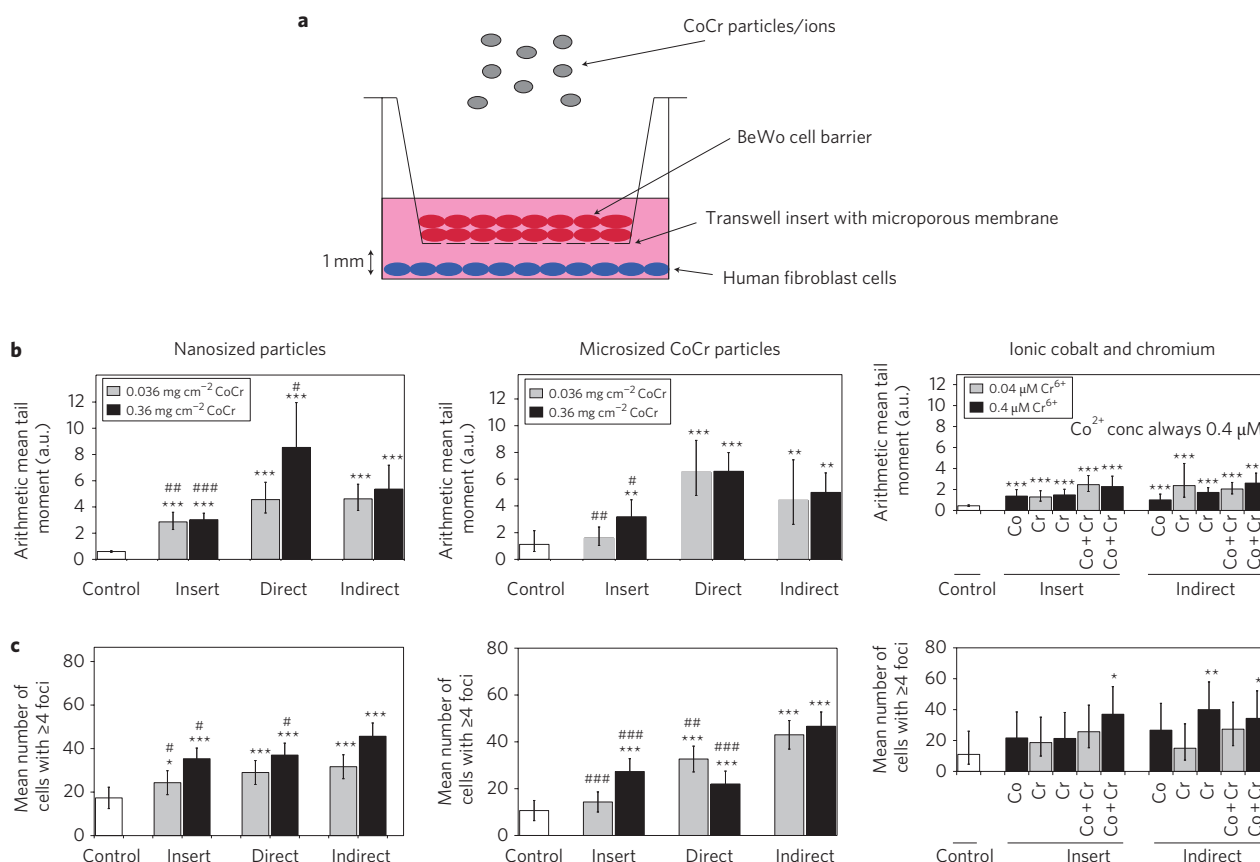


Figure 1 | CoCr particles and their respective ions cause DNA damage in human fibroblasts. **a**, Schematic showing the exposure setup. BeWo cells form a confluent cell barrier on a transwell insert above a layer of human fibroblasts. **b,c**, Fibroblasts were exposed to nano-, micrometre-sized and Co(II) and Cr(VI) ions for 24 h either through the BeWo cell barrier (indirect), through the insert without the BeWo barrier (insert) or directly onto fibroblasts without a BeWo barrier or insert (direct). Exposures were compared with fibroblasts with no CoCr exposure (control). Fibroblast DNA damage as recorded with the alkaline comet assay (**b**) and γ -H2AX assay (**c**) show that indirect exposures of all particles and ions caused significant damage when compared with the control. Damage after indirect exposures of particles (but not ions) is greater than that after exposures through inserts. All values are means \pm 95% CI (confidence interval). * $P \leq 0.05$, ** $P \leq 0.01$, *** $P \leq 0.001$ when compared with control. # $P \leq 0.05$, ## $P \leq 0.01$, ### $P \leq 0.001$ when compared with indirect exposures.

detects alkaline labile sites, single-strand and double-strand breaks, was similar to or less than that observed after direct exposures (Fig. 1b). The level of damage after indirect exposure when measured using γ -H2AX staining to measure double-strand breaks was similar to or greater than that observed after direct exposure of the fibroblasts to the CoCr particles at the same concentrations (Fig. 1c).

Significantly, fibroblast DNA damage in the presence of the BeWo layer was greater than that determined after exposure of the cells to CoCr particles placed behind the transwell plastic insert (pore size, 0.4 μ m) in the absence of the cellular barrier (Fig. 1b,c (insert)), indicating that the BeWo barrier cells contributed to the process of DNA damage. Moreover, there was no evidence of a change in permeability or electrical resistance (a measure of tight junctions¹⁸) of the barrier except for a slight change at the highest concentration of nanoparticles (Supplementary Fig. S1a,b). For this reason, all further exposures with nanoparticles were made at the lower concentration, with continued monitoring of barrier function in every experiment.

Corresponding live-cell imaging of human fibroblasts that had been directly or indirectly exposed to CoCr particles showed marginal differences in the frequency of cell deaths, although the directly exposed cells showed a reduced frequency of mitoses (Supplementary Fig. S2, Supplementary Movies S1, S2 and S3). When directly exposed fibroblasts encountered clumps of nanoparticles on the cover-glass surface, these were drawn up over the cell surfaces by retrograde actin flow, and accumulated over time to form much larger, phase bright aggregates. No other changes in

behavioural or morphological responses in the fibroblasts were seen with live cell imaging up to 48 h after exposure.

Behaviour of particles in the BeWo barrier

Transmission electron microscopy (TEM) studies showed no morphological evidence of cell death in the BeWo cellular barrier on exposure to the CoCr particles (Fig. 2a). More than 95% of the nanoparticles were located within the cells of the superficial layer of the 3- to 4-cell-thick barrier after 24 h of exposure (Fig. 2a), indicating that the CoCr particles were internalized by the BeWo cells and did not traverse the barrier. Furthermore, the micrometre-sized CoCr particles (mean size, 2.9 μ m), were too large to pass through the 0.4- μ m-wide pores of the transwell insert, but nonetheless caused substantial indirect DNA damage in the fibroblasts. Mass spectroscopic analyses of the medium below the barrier (in the absence of fibroblasts) revealed the presence of low concentrations of cobalt and chromium ions, indicating that metal ions, on the other hand, were able to cross the cellular barrier after particle exposure (Fig. 2d). Interestingly, exposure to aqueous cobalt and chromium ions in the absence of the CoCr particles did not result in transport across the BeWo cellular layer (data not shown), suggesting that corrosion of the particles inside the barrier cells was responsible for metal-ion transport into the fibroblast medium.

In support of this mechanism, the increase in cobalt concentration (from 69.2 to 87.1 ppb) in the medium below the particle-exposed barrier was much larger than the increase of

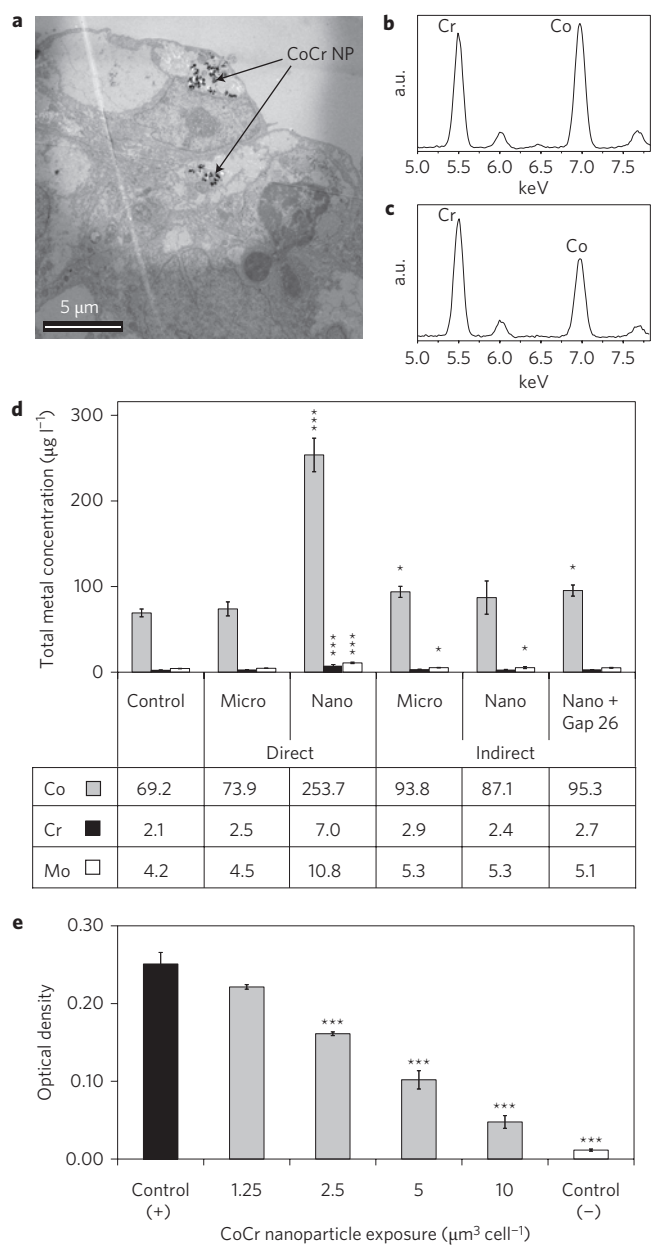


Figure 2 | Behaviour of CoCr particles in the BeWo cell barrier. **a**, TEM image of a nanoparticle-treated BeWo cell barrier showing aggregates of CoCr nanoparticles (NP) internalized in the upper layers of the barrier. **b,c**, Energy-dispersive X-ray analyses of native CoCr nanoparticles (**b**) and those inside BeWo cells (**c**) show reduced cobalt peak intensity (concentration) after the addition to BeWo cells. **d**, Concentrations of cobalt, chromium and molybdenum in fibroblast-containing media after direct exposure (direct), and in media beneath the BeWo barrier in the absence of fibroblasts (indirect) after 24 h exposure of micrometre- and nanosized CoCr particles and nanoparticles with Gap 26 placed above the barrier. Values are means \pm s.d.; * $P \leq 0.05$, *** $P \leq 0.001$ compared with controls ($n = 3$). **e**, WST-1 assay shows a dose-dependent reduction in mitochondrial metabolic activity in the BeWo cells after CoCr nanoparticle exposure. Values are means \pm s.d. *** $P \leq 0.001$ compared with control ($n = 3$).

chromium (from 2.1 to 2.4 ppb) or molybdenum (from 4.2 to 5.3 ppb) (comparing indirect exposures with control, Fig. 2d). This relative excess of cobalt does not correspond with the composition of the CoCr alloy, which was 60% cobalt, 30% chromium and

5% molybdenum. Furthermore, energy-dispersive X-ray (EDX) analysis of nanoparticles located inside BeWo cells of the superficial layer showed a 30% relative reduction in the cobalt peak intensity compared to the native nanoparticles, with no change in the chromium peak (Fig. 2b,c), and TEM images revealed roughening of the distinct shape of the native CoCr particles after internalization (data not shown). The differences in ion concentrations in the medium after direct exposures of the fibroblasts (Fig. 2d) might reflect known differences in the internalization and corrosion of micrometre-sized and nano-sized particles within fibroblasts^{20,32}.

Although the BeWo barrier cells showed no morphological evidence of cell death or changes in permeability or electrical resistance, a dose-dependent reduction of WST 1 (a marker of succinate dehydrogenase) was observed in individual BeWo cells after 24 h of nanoparticle exposure (Fig. 2e). This suggested the advent of mitochondrial toxicity without cytotoxicity, as has been reported in human fibroblasts exposed directly to CoCr¹⁶ and silver²¹ nanoparticles. Nanoparticles have been shown to aggregate in the mitochondria of human cells^{21,22}.

Origin of fibroblast DNA damage

Our results suggest an important role for the BeWo barrier in the DNA damaging process. We therefore explored the possibility of whether the fibroblast DNA damage originated from intercellular signalling pathways associated with the intact BeWo barrier. In this regard, a network of tight junctions, gap junctions and desmosomes between the BeWo cells were observed by TEM (Supplementary Figs S3,S4). Gap junctions are known to be a universal tool of intercellular communication that supports the bidirectional transport of ions, small molecules and metabolites across cells^{23,24}. Recent interest has also focused on hexameric unpaired hemichannels made of connexins or pannexins as further sources of intercellular signalling. To test the role of connexin gap junctions or hemichannels in the signalling process, we first confirmed that the BeWo cells expressed connexin 43 (Cx43; Fig. 4a). We then used the connexin mimetic peptides, Gap 26 and Gap 27, as specific blockers of gap junctions/hemichannels, and 18 α -glycyrrhetic acid as a less specific blocking agent²⁴. We also used a heptapeptide AAP10, an analogue of ZP123, an antiarrhythmic peptide, to increase gap junction communication as well as Cx43 expression²⁵. Significantly, applying gap junction blockers above (Fig. 3a–c) or below (Gap 27 but not Gap 26, Fig. 3d–f) the BeWo cellular barrier during a low-dose nanoparticle exposure above the barrier prevented DNA damage in the fibroblasts, including double-strand breaks (Fig. 3g). The indirect exposure to nanoparticles caused an increase in tetraploidy in the fibroblasts (Fig. 3h) with no increase of dicentric chromosomes or chromosome translocations, and no statistically significant increase of aneuploidy or chromosome breaks. This increase in tetraploidy was also prevented by Gap 26 (Fig. 3h). Moreover, AAP10, which increases connexin expression and ATP release^{25,26}, increased the DNA damage (Fig. 3i). In each case, no change in the integrity of the barrier was observed after these procedures when measured by dye transport or electrical resistance (Supplementary Fig. S1c,d).

Similar experiments were undertaken to determine if additional or complementary signalling pathways involving pannexin channels were operational in the BeWo cellular barrier. BeWo cells were shown to express P2X receptors (P2X2 to P2X7) and pannexin channel 1 (Fig. 4a), and addition of the pannexin channel blocker, Panx1²⁷, or the P2X7 antagonist, compound 17 (refs 27,28), to the fibroblast-containing medium during indirect exposure to CoCr nanoparticles resulted in a decrease in DNA damage to the fibroblasts (Fig. 4b,c).

As ATP can act as an extracellular signalling molecule²⁹, and is known to pass across gap junctions and hemichannels^{24,27}, we investigated the possibility that ATP could be a signalling molecule from any connexin or pannexin channels located at the base of the BeWo barrier

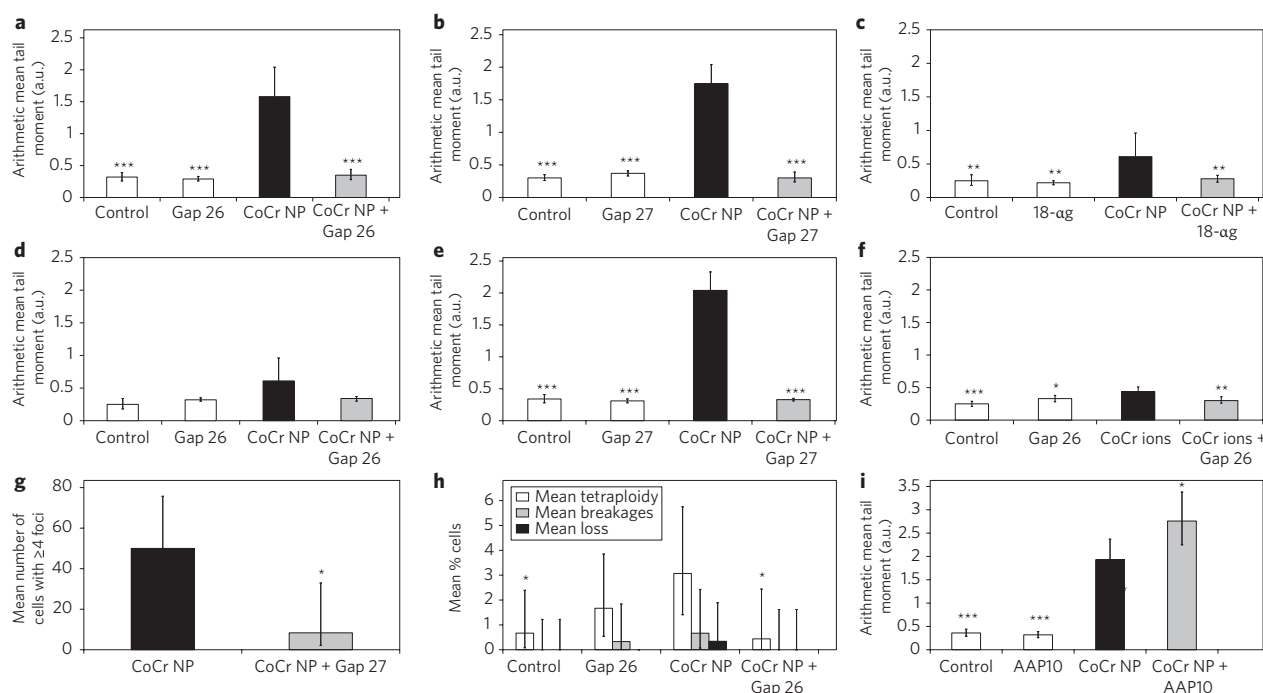


Figure 3 | Fibroblast DNA damage after indirect exposure through the BeWo barrier is dependent on intercellular signalling through connexin channels within the barrier. **a–e**, DNA damage (alkaline comet assay) to human fibroblasts after indirect exposure to CoCr nanoparticles, with Gap 26 (**a**), Gap 27 (**b**) and 18- α g (**c**) applied above the BeWo barrier, and Gap 26 (**d**) and Gap 27 (**e**) applied below the barrier. **f**, DNA damage (alkaline comet assay) after indirect exposure to Co(II) and Cr(VI) ions, with Gap 26 applied below the barrier. **g**, DNA damage (γ -H2AX assay) after indirect exposure to CoCr nanoparticles with Gap 27 applied above the BeWo barrier. **h**, Chromosomal aberrations (three-colour fluorescent *in situ* hybridization) after indirect exposure to CoCr nanoparticles with Gap 26 applied below the BeWo cell barrier. **i**, DNA damage (alkaline comet assay) after exposure to CoCr nanoparticles with AAP10 applied below the BeWo barrier. All values are means \pm 95% CI; * $P \leq 0.05$, ** $P \leq 0.01$, *** $P \leq 0.001$ compared with CoCr nanoparticles ($n = 3$).

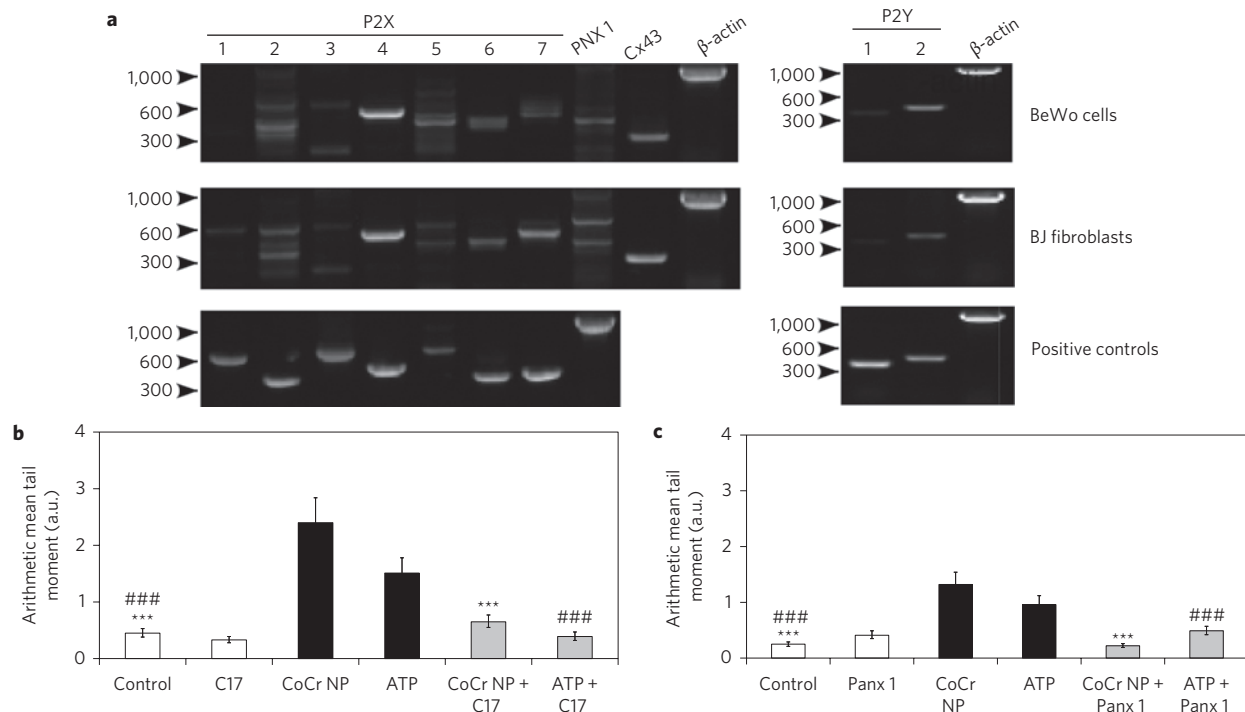


Figure 4 | DNA damage caused by either indirect exposure to CoCr nanoparticles or direct exposure to ATP (beneath the barrier) is dependent on pannexin channel signalling. **a**, Reverse transcriptase polymerase chain reaction shows that BeWo cells express mRNA for connexin 43 (Cx43), pannexin, P2Y and all P2X receptors except P2X1. Fibroblasts express mRNA for Cx43, pannexin, P2Y and all P2X receptors. **b**, DNA damage after indirect exposure to CoCr nanoparticles alone and in the presence of compound 17 (C17), and direct exposure to ATP alone and in the presence of C17 beneath the barrier. **c**, DNA damage after indirect exposure to CoCr nanoparticles alone and in the presence of pannexin mimetic peptide (Panx 1), and direct exposure to ATP alone and in the presence of the Panx 1 beneath the barrier. All values are means \pm 95% CI. *** $P \leq 0.001$ compared with CoCr nanoparticles. #### $P \leq 0.001$ compared with ATP.

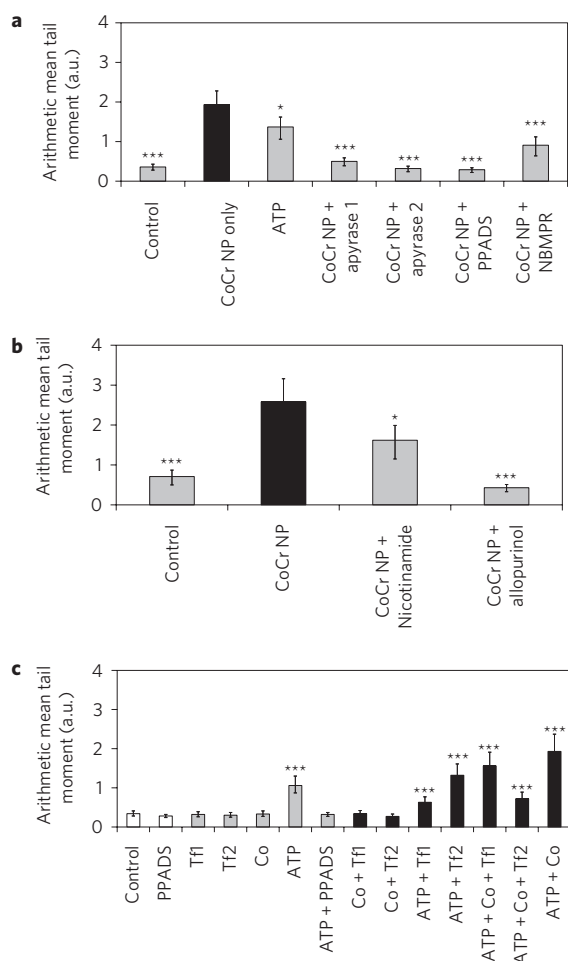


Figure 5 | ATP, transferrin and Co(II) as signals passing through the barrier. a,b, DNA damage (alkaline comet assay) to fibroblasts after indirect exposure to CoCr nanoparticles is significantly reduced by (a) apyrase 1 (A7646, Sigma-Aldrich) and 2 (A6535, Sigma Aldrich; lower ATPase/ADPase ratio), and PPADS, and by (b) NBMPR, nicotinamide and allopurinol. c, ATP but not cobalt, holo-transferrin (Tf1) or apo-transferrin (Tf2) causes DNA damage to human fibroblasts when applied directly (no barrier, no insert). This damage is blocked by the P2 receptor antagonist PPADS. All values are means \pm 95% CI. * $P \leq 0.05$, *** $P \leq 0.001$ compared with CoCr nanoparticles (a and b) and compared with controls (c).

and contribute to the DNA damage observed in the fibroblast cells. To test this we placed ATP below the BeWo cell barrier and showed that DNA damage could be induced in the fibroblasts (Figs 4b,c and 5a,c). Significantly, DNA damage in the fibroblasts indirectly exposed to CoCr nanoparticles was decreased when apyrase (an enzyme hydrolysing ATP), PPADS (which blocks the P2 purinergic receptor), NBMPR (inhibiting ATP uptake or release) or allopurinol (which inhibits xanthine oxidase) were added below the BeWo cell barrier (Fig. 5a,b). The blockade of NAD with nicotinamide was also partly effective (Fig. 5b). Like the indirect DNA damage caused by nanoparticles, the DNA damage induced by placing ATP below the BeWo cell barrier was reduced by the pannexin channel blocker, Panx 1, or the P2X7 antagonist, compound 17.

As purinergic transmission can lead to calcium wave propagation, we undertook calcium assays after ATP addition to isolated BeWo cells (similar experiments using an intact BeWo barrier with or without nanoparticle exposure were not performed owing to major technical difficulties). A strong ATP-dependent spike in calcium concentration was observed after ~ 50 s, which was P2Y (but not P2X7) receptor dependent (Supplementary Fig. S5a,b).

Moreover, DNA damage in fibroblasts associated with indirect exposure to CoCr nanoparticles was reduced by the presence of either cyclosporin A or FK506 added to the medium above the cellular barrier (Supplementary Fig. S5c). These molecules are immunosuppressive compounds that exert their effect by binding to cyclophilin A and inhibiting calcineurin³⁰, a protein phosphatase that is a critical component of several calcium-dependent signalling pathways³¹.

The above results suggest that exposure of the confluent BeWo cell layer to a low dose of CoCr nanoparticles generates signalling responses within the barrier that involve connexin and/or pannexin channels and associated ATP release^{32,33}. The connexin mimetic peptide, Gap 26, had no effect on the transport of cobalt or chromium ions through the barrier (see Fig. 2d), but it did significantly decrease the level of fibroblast DNA damage (Fig. 3). It therefore seems unlikely that DNA damage was related to the presence of metal ions in the medium. Besides, direct exposure of fibroblasts to Co(II) at 20 ppb did not cause DNA damage or augment damage initiated by ATP (see Fig. 5c). The direct action of ATP was blocked by the P2 receptor antagonist, PPADS, suggesting that it was receptor-mediated (Fig. 5c).

A search for additional candidate molecules for fibroblast DNA damage was made using two-dimensional proteomics in serum- and fibroblast-free media presented below the nanoparticle-exposed BeWo barrier (Supplementary Fig. S6). In fact, only bovine transferrin (derived from the original media used to culture the BeWo cells) was identified. This protein appeared after ATP treatment below the barrier in the absence of CoCr, and was absent when ATP activity was blocked by Gap 26, PPADS or apyrase after nanoparticle exposure (Supplementary Fig. S6). However, this protein had no influence on fibroblast DNA damage when directly applied to fibroblasts (Fig. 5c).

The outcome of this indirect exposure, the increase in tetraploidy and DNA damage without an overall change in cell proliferation, is different from that of a direct exposure to nanoparticles at the same dose. Here, there is an increase of aneuploidy and a slowing of the cell cycle³⁴. This suggests a different mechanism. Direct nanoparticle toxicity to DNA is thought to be caused by oxidative damage, including that from free radicals generated from the reactive particle surfaces and by the creation of chemical DNA adducts³⁵.

We suggest a mechanism (Fig. 6) for the indirect manner in which the top layer of the BeWo cell barrier is damaged, perhaps through nanoparticle/metal damage to mitochondria^{20,36}, or from hypoxic mimicking actions of cobalt ions³⁷, or mechanical stress to the mechanosensitive pannexin or connexin channels³⁸ in the uppermost layer of the BeWo cell barrier. These may cause ATP release from the top layer, which activates P2Y receptors of the second non-metal damaged layer in conjunction with possible gap junction intercellular communication. This in turn triggers calcium-mediated signalling, with the subsequent release of secondary messengers including ATP through connexin and pannexin hemichannels located at the bottom layer of the BeWo cell barrier, as well as altered exocytosis (as suggested by the appearance of (bovine) transferrin). As such, our model shares some similarities with other models of secondary responses to injury such as that proposed by Shestopalov and Panchin²³ (see Fig. 3 in that paper) to explain the mechanism by which ischaemia leads to vascular dilatation.

Our proposed mechanism also shows some similarities to that proposed for the radiation-induced bystander effect³⁹. Cells exposed to low-dose radiation send a signal to non-irradiated cells, causing an induction of chromatid aberrations, gene mutations in nuclear and mitochondrial DNA, micronuclei and loss of clonogenic survival³⁹. This effect is also thought to be mediated either by gap junction communication or by a signal secreted into the culture medium that may be passed on by medium transfer³⁹. In the

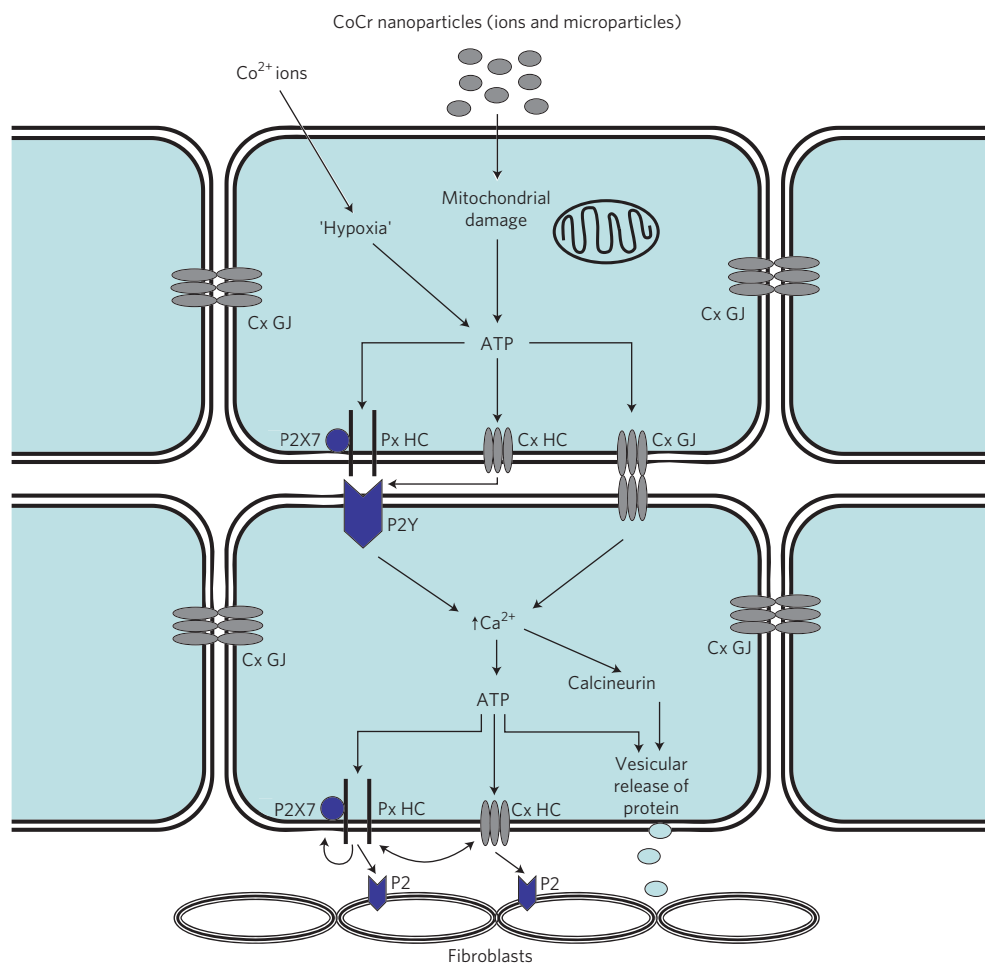


Figure 6 | Schematic of the proposed mechanism by which CoCr nanoparticles cause DNA damage to human fibroblasts across a BeWo cell barrier.

CoCr nanoparticles cause damage to mitochondria in the top layer of the BeWo barrier. Co^{2+} ions may mimic hypoxic conditions in the top layer of the BeWo barrier. Both these conditions cause a release of ATP that can pass through P2X receptors, connexin (Cx) and pannexin (Px) hemichannels (HC) to act on P2Y receptors in the second layer, or pass through connexin gap junctions (Cx GJ) and into the second layer of cells. In the second layer of the barrier, ATP (either directly or via P2Y receptor activation) causes a rise in intracellular calcium and a subsequent ATP secretion, again via connexin and pannexin hemichannels. This ATP then causes DNA damage to human fibroblasts beneath the barrier via P2 receptors on the fibroblasts.

radiation-induced bystander effect these two mechanisms are thought to represent separate channels of communication⁴⁰. However, in our experiment these lines of communication may be integrated within the same system. Our BeWo barrier, 3 to 4 cells in thickness, was not intended as a replica of the human placenta. Instead, we aimed to create a multilayered barrier devoid of gaps (such as might have been created by toxic effects of metals or in certain circumstances by syncytialization¹⁸) so that the indirect effects of nanoparticle exposure could be tested with confidence. However, we note that in the first trimester in human pregnancy the villous trophoblast comprises two layers, a layer of syncytiotrophoblast (as a syncytium in contact with the maternal blood) that rests on a second layer of cytotrophoblast^{41,42}. These two layers are interconnected by a dense punctate array of Cx43 protein in keeping with gap junctions that link the syncytiotrophoblast to the cytotrophoblast and cytotrophoblast to other cytotrophoblast⁴³. Communication through gap junctions appears to be important in placental function and development⁴⁴.

In this context it is feasible that a process of indirect DNA damage mediated through Cx43 gap junctions in a multilayered barrier might have potential relevance to the human placenta, because it is in the first trimester that the embryo may be particularly vulnerable to teratogenic effects⁴⁵. Maternal and other extra-embryonic pathways have been suggested to modulate reactive oxygen species (ROS)-mediated

teratogenesis through the production of diffusible factors that alter embryonic determinants of oxidative macromolecular damage or signal transduction⁴⁶. Excess free iron in the fetus, as transported across the placenta by transferrin⁴⁷, also contributes to oxidative stress⁴⁶, which may damage fetal organs as part of 'oxygen free radical disease of neonatology'. Tetraploidy as seen in our experiments can be associated with malformation⁴⁸.

Conclusion

In summary, we show that nanoparticles may cause damage to DNA and chromosomes across an intact cellular barrier. The nanoparticles did not pass through the barrier; instead the damage was mediated by a novel mechanism involving pannexin and connexin hemichannels and gap junctions and purinergic signalling.

Nanoparticles are increasingly being used in medicine, and their retention in the systemic circulation as a result of them being too large to be excreted through the kidneys is being used as an advantage in increasing specific targeting of organs such as the brain for therapeutic purposes. This retention, however, will lead to increased exposure of other organs. We suggest that an evaluation of nanoparticle safety should not rely on whether they fail to gain access to privileged sites. Instead there should also be an evaluation of their genotoxic potential for both direct and indirect effects to avoid any potential risks to targets on the distal side of cellular barriers.

Methods

Reagents. The reagents used were Gap 26 (300 μM) connexin mimetic peptide (VCTDKSFISHUR) (Sigma Genosys, UK), 18 α -glycyrrhetic acid (10 μM , Sigma), AAP10 (50 nM; kindly provided by J. S. Petersen, Zealand Pharma), Gap 27 (300 μM) connexin mimetic peptide (SRPTEKTIFFI), compound 17 (1 μM), Panx 1 (400 μM) peptide (Cambridge Bioscience), and ATP (10 μM), apyrase (2 units ml^{-1}), NBMPr (10 μM), PPADS (20 μM), allopurinol (50 μM), FK506 (0.2 μM), cyclosporin A (0.2 μM), nicotinamide (6 mM), $\text{K}_2\text{Cr}_2\text{O}_7$ and CoCl_2 (Sigma-Aldrich).

Methods. Human fibroblasts were exposed to nanoparticles or micrometre particles of surgical CoCr alloy (0.036 mg cm^{-2} and 0.36 mg cm^{-2}) or ions of cobalt and/or Cr(vi) (0.4 μM , 0.004 μM) (for 24 h) either directly or indirectly through a BeWo cell barrier that was 3 cells thick. Nanoparticles (29.5 \pm 6.3 nm) were generated using a flat pin-on-plate tribometer¹⁶. Artificial micrometre-sized CoCr particles (2.9 \pm 1.1 μm) were obtained from Osprey Metals. Pre-exposure particles were washed in 100% ethanol then heat sterilized at 180 $^\circ\text{C}$ for 4 h and sonicated.

Cell culture. BeWo b30 cells were obtained from Dr A. Schwartz (Washington University) and cultured in Dulbecco's modified eagle's medium (DMEM) nutrient mixture F-12 Ham with phenol red, supplemented with 1% L-glutamine-penicillin-streptomycin (PSLG), 1% amphoterin B solution (AmpB) and 10% fetal bovine serum (FBS, Sigma-Aldrich) at 37 $^\circ\text{C}$ in 5% CO_2 . BeWo cells were seeded at 1×10^5 cells cm^{-2} on polyester 0.4- μm -pore membranes in a Transwell plate and grown as a barrier with regular medium change for 7 days.

Primary BJ human fibroblasts were maintained in minimal essential medium (Sigma), supplemented with 10% FBS (Invitrogen), 2% HEPES buffer (Sigma), 1% sodium pyruvate solution (Sigma), 1% pen/strep solution (Sigma) and 1% L-glutamine (Sigma).

Analysis of fibroblasts. Fibroblasts were plated at 5×10^4 into 12-well plates (Orange Scientific) for the comet assay, and on round 18-mm glass coverslips for γ -H2AX and fluorescent *in situ* hybridization (FISH) assays.

The alkaline comet assay was performed according to previous protocols^{16,32}. Electrophoresis was performed at 4 $^\circ\text{C}$ in light-controlled conditions. A total of 100 cells for each treatment (nine repetitions) were scored at $\times 400$ magnification using a fluorescence microscope (Olympus BX-50) with an excitation filter of 515–560 nm and barrier filter of 590 nm and image analysis software (COMET III, Perceptive Instruments). DNA damage was evaluated by the tail moment (product of comet length and tail intensity).

The fibroblasts were fixed in 4% formaldehyde and immunostained with polyclonal antibody to histone γ -H2AX and donkey anti-rabbit IgG, secondary antibody. Cells with four or more foci out of 100 cells were scored in triplicate using an Olympus BX-41 microscope with image analysis software.

Chromosomes 1, 2 and 3 were 'painted' using FISH⁴⁹. Numerical and structural chromosomal aberrations were scored in 300 metaphase spreads per experiment using an Olympus BX-41 microscope equipped with single band-pass filter (Olympus) and a tri band-pass filter. Images were captured with a Cytovision digital-imaging system (Applied Imaging).

Live cell imaging of fibroblasts was performed in multiple fields in 12-well plates. Their expression of connexin and pannexins were determined using reverse transcriptase polymerase chain reaction (RT-PCR; see Supplementary Methods).

Analysis of the BeWo barrier. The integrity of the barrier was checked by measuring transepithelial electrical resistance (TEER) and the passage of sodium fluorescein and fluorescein isothiocyanate (FITC)-labelled dextrans across the barrier (see Supplementary Methods). Barriers were examined with TEM and scanning electron microscopy (SEM) with EDX analysis (see Supplementary Methods). Connexin and pannexin expressions within the barriers were analysed with RT-PCR, and calcium signalling within individual BeWo cells was performed using the Fura-2 calcium assay (see Supplementary Methods). Estimation of mitochondrial function within nanoparticle-exposed BeWo cells was made using the WST-1 assay (see Supplementary Methods).

Analysis of media. Chromium and cobalt ($\mu\text{g ml}^{-1}$), were measured using high-resolution inductively coupled plasma mass spectrometry¹⁶ by Analytica (detection limits 0.5 $\mu\text{g ml}^{-1}$).

The protein content was investigated using two-dimensional gel electrophoresis and mass spectrometry (see Supplementary Methods).

Statistical methods. Arithmetic mean comet tail moments and metal concentrations were compared between treatment groups using linear regression on the logs of the data to define confidence intervals for geometric means (GMs) of arithmetic mean tail moments and of the various metal concentrations, and to define confidence intervals and *P*-values for between-treatment GM ratios, using equal-variance standard errors. Numbers of cells in a sample with four or more γ -H2AX foci were compared between treatment groups using generalized linear models, with a binomial variance function, a log link function, and quasi-likelihood standard errors based on a dispersion parameter estimated from the Pearson χ^2 , to define confidence intervals for mean proportions of cells with four or more foci, and confidence intervals and *P*-values for the between-treatment ratios of these means⁵⁰.

Numbers of cells with aberrations in the FISH assay were compared between treatment groups using odds ratios, with hypergeometric confidence intervals and Fisher's exact *P*-values.

Received 16 July 2009; accepted 21 September 2009;
published online 5 November 2009

References

- Tiede, K. *et al.* Detection and characterization of engineered nanoparticles in food and the environment. *Food Addit. Contam.* **25**, 795–821 (2008).
- Asiyanbola, B. & Soboyejo, W. For the surgeon: an introduction to nanotechnology. *J. Surg. Educ.* **65**, 155–161 (2008).
- Park, J. H. *et al.* Biodegradable luminescent porous silicon nanoparticles for *in vivo* applications. *Nature Mater.* **8**, 331–336 (2009).
- Sajja, H. K. *et al.* Development of multifunctional nanoparticles for targeted drug delivery and noninvasive imaging of therapeutic effect. *Curr. Drug Discov. Technol.* **6**, 43–51 (2009).
- Faraji, A. H. & Wipf, P. Nanoparticles in cellular drug delivery. *Bioorg. Med. Chem.* **17**, 2950–2962 (2009).
- Nel, A., Xia, T., Madler, L. & Li, N. Toxic potential of materials at the nanolevel. *Science* **311**, 622–627 (2006).
- Nanoscience and Nanotechnologies: Opportunities and Uncertainties* (The Royal Society, London, 2004); available at <www.royalsoc.ac.uk/policy>.
- Bosman, S. J. *et al.* Development of mammalian embryos exposed to mixed-size nanoparticles. *Clin. Exp. Obstet. Gynecol.* **32**, 222–224 (2005).
- Stone, V., Johnston, H. & Clift, M. J. Air pollution, ultrafine and nanoparticle toxicology: cellular and molecular interactions. *IEEE Trans. Nanobiosci.* **6**, 331–340 (2007).
- Seaton, A. & Donaldson, K. Nanoscience, nanotoxicology and the need to think small. *Lancet* **365**, 923–924 (2005).
- Stern, S. T. & McNeil, S. E. Nanotechnology safety concerns revisited. *Toxicol. Sci.* **101**, 4–21 (2008).
- Myllynen, P. K. *et al.* Kinetics of gold nanoparticles in the human placenta. *Reprod. Toxicol.* **26**, 130–137 (2008).
- Singh, S. & Nalwa, H. S. Nanotechnology and health safety—toxicity and risk assessments of nanostructured materials on human health. *J. Nanosci. Nanotechnol.* **7**, 3048–3070 (2007).
- Keegan, G. M., Learmonth, I. D. & Case, C. P. Orthopaedic metals and their potential toxicity in the arthroplasty patient: a review of current knowledge and future strategies. *J. Bone Joint Surg. Br.* **89**, 567–573 (2007).
- Case, C. P. *et al.* Widespread dissemination of metal debris from implants. *J. Bone Joint Surg. Br.* **76**, 701–712 (1994).
- Papageorgiou, I. *et al.* The effect of nano- and micron-sized particles of cobalt-chromium alloy on human fibroblasts *in vitro*. *Biomaterials* **28**, 2946–2958 (2007).
- Drewlo, S., Baczyk, D., Dunk, C. & Kingdom, J. Fusion assays and models for the trophoblast. *Methods Mol. Biol.* **475**, 363–382 (2008).
- Liu, F., Soares, M. J. & Audus, K. L. Permeability properties of monolayers of the human trophoblast cell line BeWo. *Am. J. Physiol.* **273**, C1596–1604 (1997).
- Parry, S. & Zhang, J. Multidrug resistance proteins affect drug transmission across the placenta. *Am. J. Obstet. Gynecol.* **196**, 476.e1–6 (2007).
- Bhat, P. & Anderson, D. A. Hepatitis B virus translocates across a trophoblastic barrier. *J. Virol.* **81**, 7200–7207 (2007).
- AshaRani, P. V., Low Kah Mun, G., Hande, M. P. & Valiyaveetil, S. Cytotoxicity and genotoxicity of silver nanoparticles in human cells. *ACS Nano*. **24**, 279–290 (2009).
- Derfus, A. M., Chan, W. C. W. & Bhatia, S. N. Intracellular delivery of quantum dots for live cell labeling and organelle tracking. *Adv. Mater.* **16**, 961–966 (2004).
- Shestopalov, V. I. & Panchin, Y. Pannexins and gap junction protein diversity. *Cell Mol. Life Sci.* **65**, 376–394 (2008).
- Evans, W. H., De Vuyst, E. & Leybaert, L. The gap junction cellular internet: connexin hemichannels enter the signalling limelight. *Biochem. J.* **397**, 1–14 (2006).
- Stahlut, M., Petersen, J. S., Hennan, J. K. & Ramirez, M. T. The antiarrhythmic peptide rotigaptide (ZP123) increases connexin 43 protein expression in neonatal rat ventricular cardiomyocytes. *Cell Commun. Adhes.* **14**, 239–249 (2006).
- Clarke, C., Williams, O. J., Martin, P. E. & Evans, W. H. ATP release by cardiac myocytes in a simulated ischaemia model. Inhibition by a connexin mimetic peptide and enhancement by an antiarrhythmic peptide. *Eur. J. Pharmacol.* **605**, 9–14 (2009).
- Pelegrin, P. & Surprenant, A. Pannexin-1 mediates large pore formation and interleukin-1 β release by the ATP-gated P2X7 receptor. *EMBO J.* **25**, 5071–5082 (2006).
- Michel, A. D. *et al.* Direct labelling of the human P2X7 receptor and identification of positive and negative cooperativity of binding. *Br. J. Pharmacol.* **151**, 103–114 (2007).
- Schwiebert, E. M. & Zsembery, A. Extracellular ATP as a signalling molecule for epithelial cells. *Biochim. Biophys. Acta* **1615**, 7–32 (2003).
- Liu, J. *et al.* Calcineurin is a common target of cyclophilin–cyclosporin A and FKBP–FK506 complexes. *Cell* **66**, 807–815 (1991).

31. Crabtree, G. R. Calcium, calcineurin and the control of transcription. *J. Biol. Chem.* **276**, 2313–2316 (2001).
32. Surprenant, A. & North, R. A. Signaling at purinergic P2X receptors. *Annu. Rev. Physiol.* **71**, 333–359 (2008).
33. Lai, C. P. *et al.* Tumor-suppressive effects of pannexin 1 in C6 glioma cells. *Cancer Res.* **67**, 1545–1554 (2007).
34. Papageorgiou, I. *et al.* Genotoxic effects of particles of surgical cobalt chrome alloy on human cells of different age *in vitro*. *Mutat. Res.* **619**, 45–58 (2007).
35. Schins, R. P. & Knaapen, A. M. Genotoxicity of poorly soluble particles. *Inhal. Toxicol.* **19**, 189–198 (2007).
36. Xia, T., Kovochich, M., Liong, M., Zink, J. I. & Nel, A. E. Cationic polystyrene nanosphere toxicity depends on cell-specific endocytic and mitochondrial injury pathways. *ACS Nano.* **2**, 85–96 (2008).
37. Baumann, M. U., Zamudio, S. & Illsley, N. P. Hypoxic upregulation of glucose transporters in BeWo choriocarcinoma cells is mediated by hypoxia-inducible factor-1. *Am. J. Physiol. Cell Physiol.* **293**, C477–485 (2007).
38. Bao, L., Locovei, S. & Dahl, G. Pannexin membrane channels are mechanosensitive conduits for ATP. *FEBS Lett.* **572**, 65–68 (2004).
39. Mothersill, C. & Seymour, C. B. Radiation-induced bystander effects and the DNA paradigm: an 'out of field' perspective. *Mutat. Res.* **597**, 5–10 (2006).
40. Ballarini, F. *et al.* Modelling radiation-induced bystander effect and cellular communication. *Radiat. Prot. Dosimetry* **122**, 244–251 (2006).
41. Huppertz, B. The anatomy of the normal placenta. *J. Clin. Pathol.* **61**, 1296–1302 (2008).
42. Kibschull, M., Gellhaus, A. & Winterhager, E. Analogous and unique functions of connexins in mouse and human placental development. *Placenta* **29**, 848–854 (2008).
43. Malassiné, A. & Cronier, L. Involvement of gap junctions in placental functions and development. *Biochim. Biophys. Acta* **1719**, 117–124 (2005).
44. Aplin, J. D., Jones, C. J. & Harris, L. K. Adhesion molecules in human trophoblast—a review. 1. Villous trophoblast. *Placenta* **30**, 293–298 (2009).
45. Warrell, D. A., Cox, T. M., Firth, J. D. & Benz, E. J. Jr *Oxford Textbook of Medicine* (Oxford Univ. Press, 2009).
46. Wells, P. G. *et al.* Molecular and biochemical mechanisms in teratogenesis involving reactive oxygen species. *Toxicol. Appl. Pharmacol.* **207**, 354–366 (2005).
47. McArdle, H. J., Anderson, H. S., Jones, H. & Gambling, L. Copper and iron transport across the placenta: regulation and interactions. *J. Neuroendocrinol.* **20**, 427–431 (2008).
48. Sagot, P. *et al.* Prenatal diagnosis of tetraploidy. *Fetal Diagn. Ther.* **8**, 182–186 (1993).
49. Doherty, A. T. *et al.* Increased chromosome translocations and aneuploidy in peripheral blood lymphocytes of patients having revision arthroplasty of the hip. *J. Bone Joint Surg. Br.* **83**, 1075–1081 (2001).
50. Hardin, J. W. & Hilbe, J. M. *Generalized Linear Models and Extensions* 2nd edn (Stata Press, 2007).

Acknowledgements

Advice and discussion was kindly provided by A. Poole and A. Halestrap (University of Bristol). Support from the Research Foundation Non-medical Committee of the charitable trusts for the University Hospitals Bristol is acknowledged.

Author contributions

C.P.C., G.B., A.S., M.S. and L.C. conceived and designed the experiments. G.B., A.S., L.C., B.F., G.L., S.D., L.H., P.V., J.L. and K.H. performed the experiments. C.P.C., G.B., A.S., L.C., M.S., W.H.E., A.-M.S., G.L., S.D., L.H., P.V., J.L. and K.H. analysed the data. M.S., W.H.E., A.M.S. and E.I. contributed materials and analysis tools. C.P.C., G.B., A.S., W.H.E. and S.M. co-wrote the paper.

Additional information

Supplementary information accompanies this paper at www.nature.com/naturenanotechnology. Reprints and permission information is available online at <http://npg.nature.com/reprintsandpermissions/>. Correspondence and requests for materials should be addressed to C.P.C.